Asymmetry of the Indian Ocean Dipole

[1]Chi-Cherng Hong, [2]Tim Li, [3]LinHo, and [4]Jong-Seong Kug

[1]Department of Science, TMUE/Taiwan,

[2]IPRC/SOEST, University of Hawaii at Manoa

[3]Department of Atmospheric Sciences, National Taiwan University

[4]Climate Environment System Research Center, Seoul National Univers

Abstract

The physical mechanism for the amplitude asymmetry of SST anomalies (SSTA) between the positive and negative phases of the Indian Ocean dipole (IOD) is investigated, using the SODA and NCAR/NCEP data. It is found that a strong negative skewness appears in the IOD east pole (IODE) in the mature phase (SON), while the skewness in the IOD west pole is insignificant. Thus, the IOD asymmetry is primarily caused by the negative skewness in IODE.

A mixed layer heat budget analysis indicates that the following two air-sea feedback processes are responsible for the negative skewness. The first is attributed to the asymmetry of the wind stress-ocean advection-SST feedback. During the IOD developing stage (JJAS), the ocean linear advection tends to enhance the mixed layer temperature tendency, while nonlinear advection tends to cool the ocean in both the positive and negative events, thus contributing to the negative skewness in IODE. The second process is attributed to the asymmetry of the SST-cloud-radiation (SCR) feedback. For a positive IODE, the negative SCR feedback continues with the increase of warm SSTA. For a negative IODE, the same negative SCR feedback works when the amplitude of SSTA is small. After reaching a critical value, the cold SSTA may completely suppress the mean convection and lead to cloud-free; a further drop of the cold SSTA does not lead to additional thermal damping so that the cold SSTA may grow faster. A wind-evaporation-SST feedback may further amplify the asymmetry induced by the aforementioned nonlinear advection and SCR feedback processes.

1. Introduction

The Indian Ocean Dipole (IOD) is a zonal mode of the inter-annual variability of the Indian Ocean SST (Saji et al. 1999; Webster et al. 1999). It appears as an east-west oriented dipole of SST anomalies (SSTA) in the Indian Ocean. A positive IOD event is defined as above-normal SSTA in the tropical western Indian Ocean and below-normal SSTA in the tropical eastern Indian Ocean (Saji et al. 1999).

Based on the previous observational (Saji et al. 1999; Webster et al. 1999; Saji and Yamagta 2003; Krishnamurth and Kirtman 2003), modeling (Li et al. 2002; Shinoda et al. 2004; Lau and Nath 2004; Zhong et al. 2005; Cai et al. 2005; Behera et al. 2006) and theoretical (Li et al. 2003) studies, one may conclude that IOD is a seasonal dependent mode whose phase is locked into the annual cycle and the Asian monsoon; as a consequence of this seasonal dependence, IOD grows rapidly in northern summer, reaches a mature phase in northern fall, and decays and transforms into a basin SST mode in subsequent northern winter and spring.

As the IOD index is defined by the SSTA difference between the west pole and the east pole, the index itself may not fully reflect the variability in the Indian Ocean (Huang and Kinter III 2001). Observations show that the SST variance in the east pole is larger than that of the west pole in the peak phase of IOD (Saji and Yamagata 2003, their Fig. 5, Hong et al. (2008). This suggests that the contribution of both the poles to the IOD index might be different.

The objective of the present study is to reveal physical mechanism responsible for the IOD amplitude asymmetry in the east pole. Many previous studies are based on the positive minus negative IOD composites, which could not address this asymmetry issue.

2. Data and definitions

The Simple Ocean Data Assimilation (SODA) product of Carton et al. (2000) for 1950-2001 is used as a major dataset for the ocean diagnosis. The SODA data have been previously used for studying the Indian and Pacific Ocean dynamics (e.g., Xie at al. 2002, An and Jin 2004, Kug et al. 2005). In addition, the NCAR/NCEP reanalysis (Kalnay et al. 1996) and NOAA reconstructed Sea Surface Temperature (Smith et al. 1996) data are used for diagnosing the surface heat fluxes and the asymmetry of SSTA. A procedure is applied to the NOAA-SST to remove a linear warming trend in the Indian Ocean (Saji and Yamagata 2003, ~ 0.5˚C 100year^{-1}). Here, the east pole (90°E-110°E,10°S-0°, hereafter IODE) and west pole (50°E-70°E,10°S-10°N, hereafter IODW) boxes are same as Saji et al (1999). The ENSO event is defined when the normalized Niño3 index in NDJ is larger than 1σ. The so-defined ENSO events are similar to Trenberth (1997).

3. Measuring the IOD asymmetry

The skewness is a measure of the asymmetry of a probability distribution function, and a value of 0 represents a normal distribution (White 1980). Here we adopt the skewness to measure the amplitude asymmetry of IOD, following An and Jin (2004). The skewness is defined as:

$$\text{Skewness} = m_3 / (m_2)^{3/2} \qquad (1)$$

where m_k is the k th moment,

$$m_k = \sum_{i=1}^{N} \frac{(x_i - \overline{X})^k}{N} \qquad (2)$$

and x_i is the i th observation (seasonal mean), $\overline{X}$ the climatological mean, and N (=52) the number of observations. The statistical significance of the skewness may be estimated if the number of independent samples is known (White 1980). Because the time series of SSTA is not statistically independent, we use a range-estimate instead. It is estimated that a confidence level of 95% corresponds to the amplitude of the skewness exceeding ± 0.67.

The distribution of the SSTA skewness in the Indian Ocean (Fig. 1) shows that there is a significant negative skewness off the coast of Sumatra, and that the skewness is insignificant over the western Indian Ocean. A further examination shows that the negative skewness in IODE is season-dependent, this is, the negative skewness in the east pole can only be identified in the mature phase of IOD (SON) and become little skewed during the IOD developing phase (JJA).

An interesting question is whether or not the negative skewness in the east pole is attributed to remote ENSO forcing, as the amplitude of El Niño is in general greater than that of La Nina. To answer this question, we remove all the ENSO events (El Niño events:1951,1957,1963,1965,1969,1972,1976,1982,1987,1991,1997; La Niña events:1950,1954,1955,1964, 1970,1971,1973,1975,1988,1998,1999) and re-calculate the skewness. It turns out that the skewness of IODE just drops a little bit (from -1 to -0.97) and still passes the statistical t-test at 95% confidence level. [In this case the threshold is a little higher due to the decreasing sample number (N=30).] The results above indicate that the negative skewness in IODE is primarily attributed to local air-sea feedback processes in the Indian Ocean.

4. Cause of the IOD asymmetry

To understand the relative roles of ocean advection and surface heat fluxes in causing the SSTA amplitude asymmetry in IODE, we analyze the oceanic mixed layer heat budget and make composites for the positive and negative SSTA events. The mixed layer temperature tendency equation may be written as (Li et. 2002):

$$\frac{\partial T'}{\partial t} = -(V' \cdot \nabla \overline{T} + \overline{V} \cdot \nabla T') - (V' \cdot \nabla T') + \frac{1}{\rho C_p H}(Q_{SW} + Q_{LW} + Q_{LH} + Q_{SH})' + R \qquad (3)$$

where T denotes the mixed layer temperature, V is three dimensional ocean current, which is defined as the vertical average from surface to the bottom of mixed layer, ∇ denotes 3 dimensional (3D) gradient operator, $(\ )'$ represents the anomaly variables, $(\ \overline{\ })$ the climatological mean variables, term $-(V' \cdot \nabla \overline{T} + \overline{V} \cdot \nabla T')$ is the summation of linear advection terms, term $-(V' \cdot \nabla T')$ denotes 3D nonlinear temperature advection term, Q_{SW}, Q_{LW}, Q_{LH}, and Q_{SH} represent the net downward shortwave radiation at the ocean surface, net downward surface long-wave radiation, surface latent and sensible heat fluxes, R represents the residual term, ρ is the density of water, C_p is the specific heat of water, and H denotes the mixing layer depth. Here, a positive heat flux indicates heating the ocean.

The composite evolution of the mixing layer temperature (hereafter MLT) and its tendency ($\partial T' / \partial t$) is illustrated in Fig. 2. Note that initial SST perturbations in May in both positive and negative events have similar amplitude, but they diverse quickly after August, and at the mature phase (October) the amplitude of MLT in the negative IODE composite is almost doubled (0.6℃) compared with that in the positive IODE composite (0.3℃). The MLT asymmetry in the mature phase is obviously attributed to the asymmetry of MLT tendency during the developing stage. From the time evolution of the MLT tendency term, one may clearly see that the maximum difference of the temperature tendency between the positive and negative composites appears in JJAS. Therefore, it is crucial to examine the dynamic and thermodynamic processes that give rise to the asymmetric MLT tendency during the developing phase.

a) Effect of nonlinear temperature advection

To understand the role of the ocean dynamics in causing the MLT tendency asymmetry, we decompose 3D ocean temperature advection into the zonal, meridional and vertical temperature advection components. Also we further decompose them into linear and nonlinear advection terms by separating the climatological annual cycle and interannual anomaly fields. The sum of both the linear and nonlinear advection terms in contributing to the asymmetric MLT tendency is shown in Fig. 3. The amplitudes of both linear and nonlinear advections are greater in the negative IODE phase than in the positive IODE phase. Note that while the linear advection terms contribute to the growth of both the positive and negative IODE, the nonlinear terms (which have the same magnitude as the linear terms) tend to cool the MLT in both the warm and cold episodes. This reveals that the nonlinear advection may play an important role in causing the negative skewness in the east pole. A further analysis indicates that both horizontal and vertical nonlinear advection terms contribute significantly to the negative skewness. The analysis above points out that the nonlinear advection is crucial in causing the IODE asymmetry (Fig. 4).

b) Effects of the wind-evaporation-SST feedback and the

cloud-radiation-SST feedback

The asymmetry of the surface heat flux anomaly is another significant contributor to the negative skewness, in addition to the nonlinear ocean advection process. Fig. 5 shows the horizontal patterns of the composite Q_{LH}, Q_{SR} and SST anomaly fields. To reflect their respective peak phase, the composite latent heat flux anomaly is taken during JJA while the net surface solar radiation anomaly is taken during SON. As expected, the latent heat flux anomaly tends to increase the cold SSTA, while the solar radiation anomaly tends to damp the SSTA. As discussed in Li et al. (2003), the effect of the evaporation-wind-SST feedback is season-dependent, and depends on the change of seasonal mean winds. It exhibits a positive feedback in boreal summer but a negative feedback in boreal winter. The cloud-radiation–SST feedback, on the other hand, always acts as a negative feedback process (Ramanathan and Collins 1991, Li et al. 2000).

To understand how the asymmetric effect of the cloud-radiation-SST feedback is resulted, we show the scatter diagram for the precipitation-SST and Q_{SR} -SST relationships as shown in Fig. 6. In general, the SSTA are positively correlated with the precipitation anomalies (r=0.76) while negatively correlated with the surface shortwave radiation anomalies (r=-0.72). However, the relationships are not simply linear. When the SSTA amplitude is relatively small, the relationships are in general linear, indicating that precipitation anomalies increase and short wave radiation anomalies decrease with increased SSTA. However, after the cold SSTA reach a certain magnitude (say, -2σ), even with continuous increase of the cold SSTA, the precipitation anomaly stops decreasing and is saturated to a critical value. Similarly the shortwave radiation anomaly is also saturated. This means that the thermodynamic damping due to the cloud radiation forcing does not work any more after the cold SSTA reach a critical amplitude. Therefore, the cold SSTA may grow faster due to lack of the thermal damping.

5. Summary and discussion

In this study we investigate the amplitude asymmetry of SSTA between the positive and negative IOD events by diagnosing the SODA and NCAR/NCEP reanalysis data. The strength of the asymmetry is measured by the concept of skewness. A mixed layer heat budget analysis is conducted to understand specific dynamic and thermodynamic mechanisms that lead to the asymmetry. The main results are summarized as below:

(1) A significant negative skewness for SSTA appears in the southeast Indian Ocean off Sumatra during the mature phase of IOD, while the near zero skewness appears in the western Indian Ocean. In addition to the negative skewness in the SSTA, the surface wind stress and thermocline depth anomalies also exhibit a significant negative skewness. The IOD amplitude asymmetry is primarily caused by the asymmetry in the east pole.

(2) The negative skewness of the SSTA in the east pole is season-dependent, and it only appears in SON, the IOD mature phase. There is no clear evidence showing that the negative skewness results from the asymmetry of remote El Niño/La Niña forcing in northern summer.

(3) The mixed layer heat budget analysis points out that the negative skewness in the east pole is mainly induced by a) anomalous nonlinear horizontal and vertical ocean temperature advection and b) the asymmetry of cloud-radiation-SSTA feedbacks between the positive and negative IOD events. The wind-evaporation-SST feedback plays a role in enhancing the amplitude asymmetry.

References

An, S.-I., and F.-F. Jin, 2004: Nonlinearity and asymmetry of ENSO. *J. Climate*, **17**, 2399-2412.

Behera, S. K., J.-J. Luo, S. Masson, S. A. Rao, H. Sakuma, and T. Yamagata, 2006: A CGCM study on the interaction between IOD and ENSO. *J. Climate*, **19**, 1688-1705.

Cai, W., H. H. Hendon, and G. Meyers, 2005: Indian Ocean dipolelike variability in the CSIRO Marks 3 coupled climate model. *J. Climate*, **18**, 1449-1468.

Carton, J., G. Chepurin, X. Cao, and B. Giese, 2000: A simple ocean data assimilation analysis of the global upper ocean 1950-95. Part I: Methodology. *J. Phys. Oceanogr.*, **30**, 294-309.

Hong, C.-C., M.-M. Lu, and M. Kanamitsu, 2008: Temporal and spatial characteristics of positive and negative Indian Ocean Dipole with and without ENSO. *J. Geophys. Res.*, ***113***, DO8107, doi:10.1029/2007JD009151.

Huang, B, and J. L. Kinter III, 2001: The interannual variability in the tropical Indian Ocean and its relation to El Niño/Southern Oscillation. COLA Tech. Report 94. Center for Ocean-Land-Atmosphere Studies, Calverton, MD, USA.

Kalnay, E., and Coauthors, 1996: The NCEP/NCAR 40-year reanalysis project. *Bull. Amer. Meteor. Soc.*, **77**, 437-471.

Krishnamurthy, V. and B. P. Kirtman, 2003: Variability of Indian Ocean: Relation to monsoon and ENSO. *Quart. J. Roy. Meteor. Soc.*, **129**, 1623-1646.

Kug, J.-S., S.-I. An, F.-F. Jin and I.-S. Kang, 2005: Preconditions for El Nino and La Nina onsets and their relation to the Indian Ocean. *Geophy. Res. Lett.* **32**, L05706, doi:10.1029/2004GL021674.

Lau, N.-C., and M. J. Nath. 2004: Coupled GCM simulation of atmosphere–ocean variability associated with zonally asymmetric SST changes in the Tropical Indian Ocean. *J. Climate*, **17**, 245–265.

Li, T., T. F. Hogan, and C.-P. Chang, 2000: Dynamic and thermodynamic regulation of ocean warming, *J. Atmos. Sci.*, **57**, 3353–3365.

Li, T., Y. Zhang, E. Lu, and D. Wang, 2002: Relative role of dynamic and thermodynamic processes in the development of the Indian Ocean dipole: An OGCM diagnosis. *Geophys. Res. Lett.*, **29**, 2110, doi:10.1029/2002GL015789.

Li, T., B. Wang, C.-P. Chang, and Y. Zang, 2003: A theory for the Indian Ocean dipole-zonal mode. *J. Atmos. Sci.*, **60**, 2119-2135.

Ramanathan, V., and W. Collins, 1991: Thermodynamic regulation of ocean warming by cirrus clouds deduced from observations of the 1987 El Niño. *Nature*, **351**,

27-32.
Saji, N. H., B. N. Goswami, P. N. Vinayachandran, and T. Yamagata,1999: A dipole mode in the tropical Indian Ocean. *Nature,* **401**, 360-363.
Saji, N. H., and T. Yamagata, 2003: Structure of SST and surface wind variability during Indian Ocean dipole mode events: COADS observations. *J. Climate*, **16**, 2735-2751.
Shinoda, T., M. A. Alexander, and H. H. Hendon, 2004: Remote response of the Indian Ocean to interannual SST variations in the tropical Pacific. *J. Climate*, **17**, 362-372.
Smith, T. M., and R. W. Reynolds, R. E. Livezey, and D. C. Stokes, 1996: Reconstruction of historical sea surface temperature using empirical orthogonal functions. *J. Climate,* **9**, 1403-1420.
Tozuka, T., J.-J. Luo, S. Masson, S. K. Behera, and T. Yamagata, 2005: Annual ENSO simulated in a coupled ocean-atmosphere model. *Dyn. Atmos. Oceans*, **39**, 41-60.
Trenberth, K. E., 1997: The definition of El Niño. *Bull. Amer. Meteor. Soc.*, **78**, 2771–2777.
Webster, P. J., A. M. Moore, J. P. Loschnigg, and R. R. Leben, 1999: Coupled ocean-atmosphere dynamics in the Indian Ocean during 1997-1998. *Nature,* **401**, 356-360.
White, H. G., 1980: Skewness, kurtosis and extreme values of Northern Hemisphere geopotential heights. *Mon. Wea. Rev.*, **108**, 1446-1455.
Xie, S.-P., H. Annamalai, F. A. Schott, and J. P. McCreary, 2002: Structure and mechanisms of South Indian Ocean climate variability. *J. Climate,* **15**, 864-878.
Yu, J.-Y., and K. M. Lau, 2004: Contrasting Indian Ocean SST variability with and without ENSO influence: A coupled atmosphere-ocean study. *Meteror. Atmos. Phys.,* **90**, doi:10.1007/s00703-004-0094-7.
Zhang, Y., W. B. Rossow, A. A Lacis, V. Oinas, and M. I. Mishchenko, 2004: Calculation of radiative fluxes from the surface to top based on ISCCP and other global data sets: Refinements of the radiative transfer model and the input data. *J. Geophys. Res.*, **109**, D19105,doi:10.1029/2003JD004457.
Zhong, A., H. H. Hendon, and O. Alves, 2005: Indian Ocean variability and its association with ENSO in a global coupled model. *J. Climate,* **18**, 3634-3649.

Figures

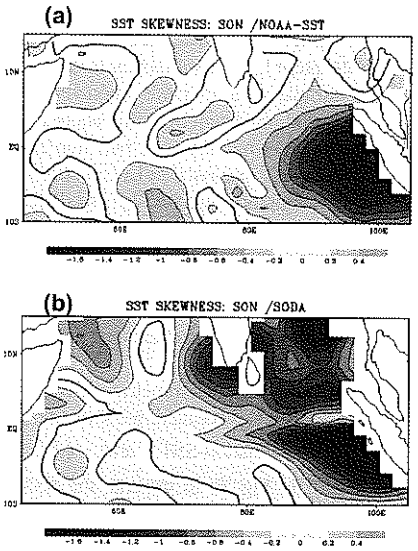

Figure 1 Distribution of the skewness of the Indian Ocean SSTA in SON for the NOAA (a) and SODA (b) data sets. The calculation is based on the data for 1950-2001.

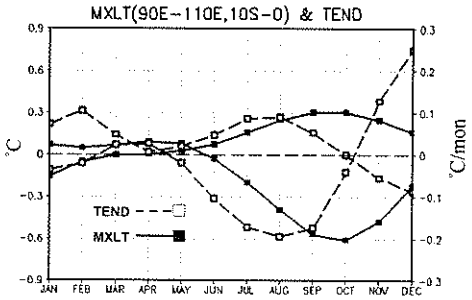

Figure 2 Composite mixed layer temperature (—■) and mixed layer temperature tendency (---□). Red (blue) lines denote the positive (negative) IODE events.

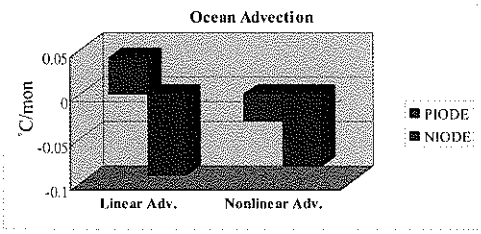

Figure 3 Relative contribution of linear advection and nonlinear advection terms in contribution to mixed layer temperature tendency in JJAS.

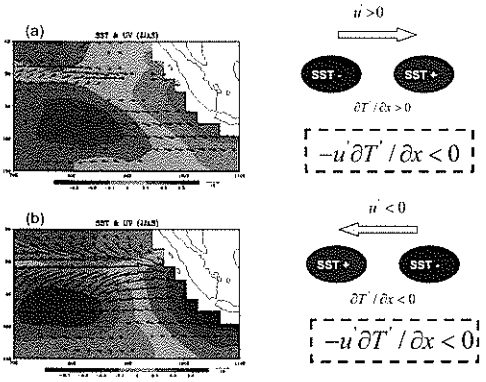

Figure 4 Left: mixed layer temperature and horizontal ocean current (z=7.5m) anomalies in JJAS for the positive and negative IODE composites. The unit vector of the ocean current is 10 cm/s. Right: schematic diagram of the nonlinear zonal advection.

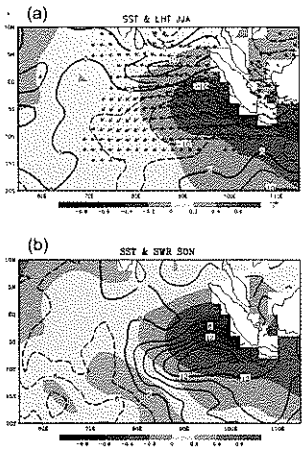

Figure 5 (a) composite SST (shaded), surface latent heat flux (contour), and 850hPa wind anomalies in JJA and (b) composite SST (shading) and net downward solar radiation (contour) anomalies in SON during the negative IODE events. The unit vector of the wind anomalies is 1 m/s. The contour intervals are 5 W/m^2 for the latent heat flux and 3 W/m^2 for the solar radiation. A positive heat flux indicates heating the ocean.

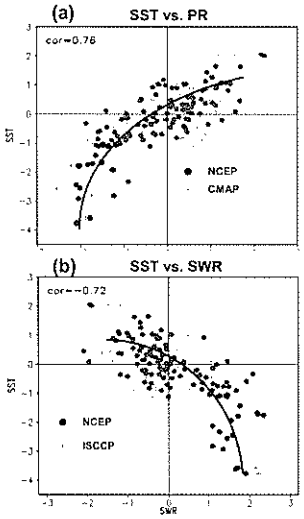

Figure 6 Scatter diagrams for the SST-precipitation (a) and SST-surface shortwave radiation (b) relationships. Monthly anomaly data in September and October are plotted in the scatter diagrams. All fields have been normalized with respect to their standard deviations. The blue dots indicate that the normalized SST and precipitation/shortwave radiation exceed one standard deviation.